

# DFAMS: Dynamic-flow guided Federated Alignment based Multi-prototype Search

Zhibang Yang<sup>1\*</sup>, Xinke Jiang<sup>1\*</sup>, Rihong Qiu<sup>1\*</sup>, Ruiqing Li<sup>1</sup>, Yihang Zhang<sup>2</sup>, Yue Fang<sup>1</sup>, Yongxin Xu<sup>1</sup>, Hongxin Ding<sup>1</sup>, Xu Chu<sup>1</sup>, Junfeng Zhao<sup>1†</sup>, Yasha Wang<sup>1†</sup>

<sup>1</sup>Key Laboratory of High Confidence Software Technologies, Ministry of Education; School of Computer Science, Peking University, Beijing, China

<sup>2</sup>Northeastern University, Shenyang, China

{yangzb,XinkeJiang,RihongQiu,YueFang}@stu.pku.edu.cn

## Abstract

Federated Retrieval (FR) routes queries across multiple external knowledge sources, to mitigate hallucinations of LLMs, when necessary external knowledge is distributed. However, existing methods struggle to retrieve high-quality and relevant documents for ambiguous queries, especially in cross-domain scenarios, which significantly limits their effectiveness in supporting downstream generation tasks. Inspired by dynamic information flow (DIF), we propose DFAMS, a novel framework that leverages DIF to identify latent query intents and construct semantically aligned knowledge partitions for accurate retrieval across heterogeneous sources. Specifically, DFAMS probes the DIF in LLMs by leveraging gradient signals from a few annotated queries and employing Shapley value-based attribution to trace neuron activation paths associated with intent recognition and subdomain boundary detection. Then, DFAMS leverages DIF to train an alignment module via multi-prototype contrastive learning, enabling fine-grained intra-source modeling and inter-source semantic alignment across knowledge bases. Experimental results across five benchmarks show that DFAMS outperforms advanced FR methods by up to 14.37% in knowledge classification accuracy, 5.38% in retrieval recall, and 6.45% in downstream QA accuracy, demonstrating its effectiveness in complex FR scenarios.

## 1 Introduction

Retrieval-Augmented Generation (RAG) leverages external knowledge documents (Edge et al. 2024; Asai et al. 2023) to effectively enhance the factuality and verifiability of outputs from Large Language Models (LLMs) (OpenAI 2022, 2023; Kaplan et al. 2020; Vu et al. 2024), significantly mitigating issues such as hallucination and knowledge obsolescence (Ji et al. 2023; Cao et al. 2020; Jiang et al. 2024b,a; Asai et al. 2024; Su et al. 2024; Jeong et al. 2024; Baek et al. 2025). However, mainstream RAG approaches typically rely on a single, centralized vector database for knowledge base selection (Kukreja et al. 2024; Bhavnani and Wilson 2009). In reality, knowledge is inherently distributed across multiple heterogeneous data sources — for instance, in medical scenarios, retrieval may need to simultaneously access

electronic health records (EHR) (Yuan, Zhou, and Yu 2023), textbooks, and the latest research papers (Zhao et al. 2025).

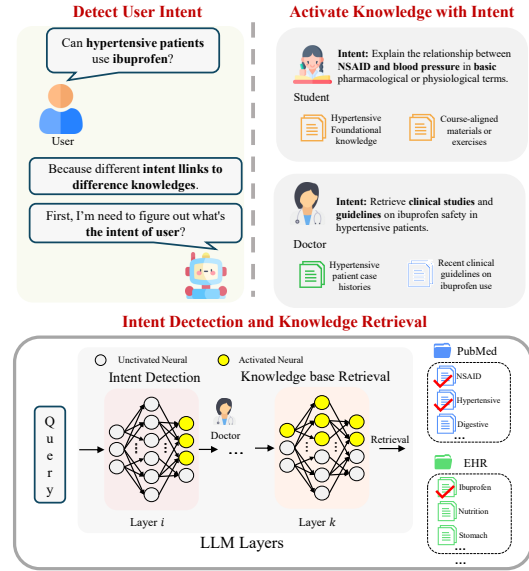


Figure 1: Since the underlying intent of different users varies, answering the same question may require distinct types of knowledge for a student and a doctor. Such differences in information needs can be reflected in the dynamic information flow within LLMs.

Forcibly aggregating all documents into a unified index not only incurs high retrieval costs but also raises concerns around data sovereignty (Jiang 2024; Shokouhi, Si et al. 2011; Kairouz et al. 2021). To address this, **Federated Retrieval (FR)** has emerged as a solution, enabling efficient cross-knowledge-base routing decisions that directly and precisely direct queries to the most relevant sources of knowledge (Schölkopf 2019; Guerraoui et al. 2025; Wang et al. 2024c; Ryan et al. 2025; Shojaee et al. 2025).

Most existing FR methods are primarily designed with an emphasis on routing efficiency, privacy preservation, and downstream task integration (Chakraborty, Dahal, and Gupta 2025). However, in real-world scenarios with complex semantics (Clarke et al. 2008), users are more con-

\*These authors contributed equally.

†Corresponding authors.

cerned with whether the system can accurately retrieve highly relevant documents to effectively support downstream generation tasks (Shokouhi, Si et al. 2011; Huang and Huang 2024), which does not receive sufficient attention in existing research. And due to limitations in current modeling strategies (Wang et al. 2024c), existing approaches exhibit notable shortcomings in addressing this issue (Guerraoui et al. 2025). On one hand, user queries often suffer from semantic ambiguity or compression, leading to a gap between surface expressions and underlying intent (Yuan et al. 2025). In different contexts, the same question may require different knowledge sources to answer (as illustrate in Figure 1). In such scenarios, user queries often fail to align with the structured and detailed content in the knowledge base, limiting the accuracy and coverage of semantic matching in traditional FR methods (Huang et al. 2021). Although some approaches leverage LLMs for prompt-based query rewriting (Gao et al. 2022) to reduce ambiguity, they often struggle to capture fine-grained semantics due to limited prompt expressiveness, leading to suboptimal performance in semantically complex scenarios. On the other hand, in real-world applications knowledge bases are typically partitioned by data sources, forming multiple structured yet interrelated knowledge subsystems (Wu et al. 2025). The semantic boundaries between these subsystems are often flooded and overlapping. However, some existing methods overlooking underlying semantic connections, which struggle to support cross-source recall and dynamic integration. (Wang et al. 2024c).

Recent research work has shown that when LLMs process tasks of different fields, the contribution of each parameter in the LLM model varies (Dhamdhere, Sundararajan, and Yan 2018; Yu et al. 2018; LeCun, Denker, and Solla 1989). Recent studies on the structural and functional mechanisms of LLMs have revealed that, during inference, LLMs naturally form a Dynamic Information Flow (DIF)—a latent path through which information propagates dynamically across transformer layers, activating neural substructures associated with semantics, knowledge, and reasoning (Zheng et al.; Yu and Ananiadou 2024; Wang et al. 2024d). These findings suggest that LLMs may already possess an implicit capability to recognize user intent and organize knowledge into latent subdomains when processing complex queries.

Recent studies have shown that LLMs exhibit functional partitioning, where different parameter groups specialize in tasks across diverse domains (Dhamdhere, Sundararajan, and Yan 2018; Yu et al. 2018; LeCun, Denker, and Solla 1989). During inference, these functional partitions associated with semantics, knowledge, and reasoning are selectively activated by the model, giving rise to Dynamic Information Flow (DIF) (Zheng et al.; Yu and Ananiadou 2024; Wang et al. 2024d; Stolfo, Belinkov, and Sachan). Inspired by this line of work, we raise a central research question: Can the dynamic information flow (DIF) within LLMs be explicitly modeled to (1) more accurately identify users’ latent query intents, and (2) structurally segment and dynamically organize overlapping or fuzzy-boundary knowledge subdomains to mitigate semantic misalignment and cross-source retrieval failures in FR settings? As shown in Fig-

ure 1, we hypothesize that, when presented with a complex query, the LLM first identifies the user’s intent. If the model determines that the user is likely a doctor with an intent to retrieve clinical studies and guidelines, it will activate the corresponding neurons, forming a reasoning pathway that generates perception signals related to the target knowledge. These signals may be used to retrieve and align content from heterogeneous sources such as PubMed and EHR, integrating cross-subdomain knowledge for downstream generation.

To validate the above hypothesis, we need to address two core challenges: (C1) how to accurately detect the relevant DIF within LLMs; (C2) how to leverage the DIF-based internal semantic organization to support fine-grained knowledge base modeling while preserving semantic associations across multiple sources. To tackle these challenges, we propose a novel framework named DFAMS (Dynamic-flow guided Federated Alignment based Multi-prototype Search). DFAMS explicitly models the internal DIF of LLMs and constructs knowledge base partitions aligned with the model’s activation patterns, thereby preserving rich semantic signals. For **Challenge C1**, we utilize gradient signals under a small number of annotated DIF-probing samples, and apply Shapley value-based attribution methods to identify neuron flow paths associated with query intent recognition and subdomain boundary detection. For **Challenge C2**, during training, we extract DIF flows induced by queries over each knowledge base. These flows are then used to train an alignment module via multi-prototype contrastive learning, achieving fine-grained intra-source modeling and inter-source alignment. The goal is to maintain semantic continuity across sources while enabling effective knowledge base classification. In summary, our contributions are as follows:

- We reveal a high-dimensional, information-rich DIF in LLMs that encodes both user intent and subdomain knowledge, enabling more faithful query understanding. To our knowledge, this is the first work to exploit FID for intent-aware, domain-sensitive retrieval modeling.
- We propose the DFAMS framework. By modeling DIF, we construct knowledge partitions that preserve inter-source semantic associations. DFAMS integrates multi-prototype contrastive learning during training and employs Adaptive Prototype-Guided Routing at inference time, significantly improving the performance.
- We develop an enhanced FR benchmark dataset to encompass more realistic and diverse query types—ranging from knowledge-free queries, multi-fragment queries within a single source, to cross-source retrieval. The benchmark integrates structured taxonomy, associated documents, user queries, and ground-truth answers, offering a solid foundation for evaluating FR in complex settings.

## 2 Related Work

### 2.1 Federated Retrieval

Federated search (Shokouhi, Si et al. 2011), extended into RAG by combining privacy-preserving federated learning (FL) (Zhang et al. 2021) with RAG (Lewis et al. 2020), enables retrieval across decentralized sources without shar-

ing raw data (Chakraborty, Dahal, and Gupta 2025), which has seen widespread adoption in privacy-critical domains such as healthcare (Jiang 2024; Jung, Jeong, and Huh 2025; Xiong et al. 2024), finance, and legal services (Addison et al. 2024). Prior work in federated search mainly targets three aspects: (i) privacy and security through secure retrieval and encryption (Jeon et al. 2021; Peng et al. 2021), (ii) retrieval efficiency via query routing (Wang et al. 2024c), and (iii) integration of FL and RAG tailored to domain-specific tasks (Wang et al. 2024a; Zeng et al. 2024; Shojaee et al. 2025). These advances have proven effective (Zhao 2024; Xu et al. 2022; Wang et al. 2024a; Zeng et al. 2024; Shojaee et al. 2025); however, retrieving high-quality results in complex semantic scenarios remains challenging (Wang et al. 2024c). Existing FR methods, prompt-based and embedding-based, struggle in this setting because queries often misalign with knowledge structures, which reduces dense vector accuracy (Huang et al. 2021), and LLM-based prompt rewriting lacks fine-grained semantic precision (Gao et al. 2022).

## 2.2 Neural Information Flow

Recent studies have shown that LLMs, like the human cortex (Arbib 2003; Hawrylycz et al. 2012; Zador 2019; Wang et al. 2024b), exhibit functional partitioning across their architecture (Dhamdhere, Sundararajan, and Yan 2018; Yu et al. 2018; LeCun, Denker, and Solla 1989). Such functional partitions may emerge in the form of attention heads (Zheng et al. 2024; Yin and Steinhardt 2025; Wu et al. 2024), feed-forward networks (Bandarkar et al. 2024; Wendler et al. 2024; Sun et al. 2025), or neurons (Huo et al. 2024; Tang et al. 2024), which are shaped during training and contribute differently across tasks (Dhamdhere, Sundararajan, and Yan 2018; Yu et al. 2018). Building on this partitions, information dynamically flows among these functional modules, forming a Dynamic Information Flow (DIF) (Stolfo, Belinkov, and Sachan; Yu and Ananiadou 2024). To leverage DIF for downstream tasks, researchers attempt to detect DIF by quantifying the attribution of parameters in the LLM with respect to input query. Quantitative attribution methods have been extensively explored using various techniques, including forward-based methods (Liang et al.; Todd et al. 2023; Jiang et al. 2025; Dai et al. 2021) and backward-based methods (Feng et al. 2025, 2024) or their combinations (Xu et al. 2024). Among these methods, Shapley value-based approaches (Ghorbani and Zou 2020; Adamczewski, Li, and van Gool 2024) have gained wide adoption. Although there has been extensive research on FIDs in large models, leveraging their powerful capabilities for modeling user intent and knowledge bases remains largely unexplored.

## 3 Method

We introduce DFAMS, a framework designed to enable LLM to perform semantically grounded FR across distributed knowledge bases, as illustrated in Figure 2. DFAMS operates in three stages: (1) formalizing the FR setting (Section 3.1); (2) extracting query-specific internal representations through *Dynamic Information Flow* (DIF) modeling (Section 3.2); and (3) aligning these representations with

structured knowledge prototypes for adaptive, multi-source routing (Section 3.3). All key notations are summarized in Appendix A.

### 3.1 Problem Definition

**Federated Retrieval Formalization.** We formulate FR as a distributed retrieval problem over  $I$  isolated data sources, where each source  $i \in \{1, \dots, I\}$  privately hosts a knowledge base  $\mathcal{K}_i = \{d_{i\ell}\}_{\ell=1}^{M_i}$  with  $M_i$  documents. Due to strict privacy constraints, sources cannot exchange raw documents or intermediate representations. Given a user query  $x$ , the system must determine a routing vector:

$$f_{\text{route}} : x \mapsto \mathbf{w} = [w_1, w_2, \dots, w_I], \quad w_j \in \mathbb{N}_0, \quad (1)$$

where  $w_j$  specifies how many documents to retrieve from  $\mathcal{K}_j$ . The challenge lies in selecting the most relevant sources adaptively while avoiding unnecessary retrieval.

**RAG in FR.** Following RAGRoute (Guerraoui et al. 2025), we combine two types of knowledge: (i) parameterized knowledge  $\Theta$  stored in the model weights, and (ii) non-parameterized knowledge  $\mathcal{D} = \{\mathcal{K}_1, \dots, \mathcal{K}_I\}$ , representing distributed, domain-specific corpora. Given a query  $x$ , the goal is to generate a reliable response:

$$\text{Response} \leftarrow \Theta(x, R \mid \mathcal{P}), \quad (2)$$

where  $\mathcal{P}$  is a task-specific prompt, and  $R$  is the subset of knowledge bases deemed relevant. To handle queries answerable without external retrieval, we include an `Others` category solved solely by  $\Theta$  (Su et al. 2024). During training, supervision is single-source: each  $(x, \mathcal{K}_i, y)$  is paired with a single knowledge base or labeled as `Others`. At inference, the model generalizes to *no-source*, *single-source*, or *multi-source* retrieval by predicting per-source relevance scores and selecting those above a dynamic threshold  $\delta$ .

### 3.2 Dynamic Information Flow Modeling

To accurately interpret user intent and uncover domain-relevant semantics for routing (**C1**), we detect *Dynamic Information Flow* (DIF) capturing which neurons contribute most to domain-sensitive behavior, producing a compact, semantically grounded representation.

The process consists of two steps: (1) constructing a controlled probing dataset to isolate domain-selection behaviors; and (2) identifying key layers and neurons via gradient-based Shapley attribution, and aggregating their activations into a DIF embedding.

**Probing Dataset Construction.** Using benchmark training or test sets for attribution often yields spurious signals, as they contain mixed user specific intents. To address this, we construct a dedicated probing dataset:

$$\mathcal{D}_{\text{probe}} = \{(x_i, \mathcal{K}_i)\}_{i=1}^{n_{\text{probe}}},$$

where each query  $x_i$  is synthesized with fixed instruction-style prompts explicitly designed to elicit domain-selection (e.g., asking the model to identify the most relevant knowledge base). Each label  $\mathcal{K}_i \in \{1, \dots, I\}$  specifies the correct knowledge base. This dataset is disjoint from  $\mathcal{D}_{\text{train}}$  and  $\mathcal{D}_{\text{test}}$  to ensure no leakage.

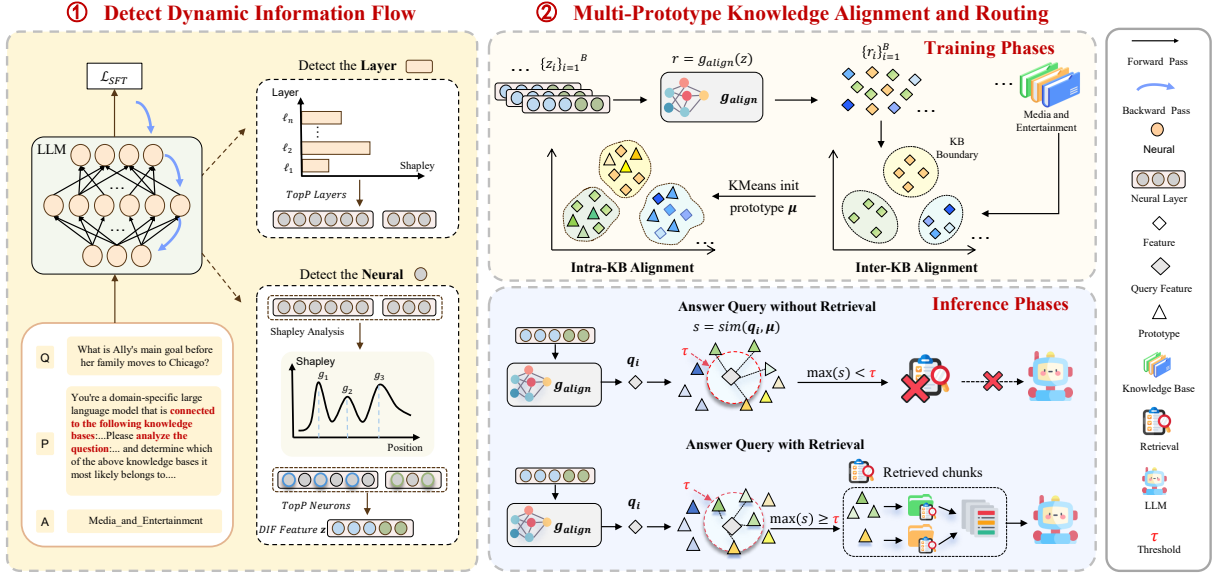


Figure 2: DFAMS dynamically detects relevant information flow in LLMs and employs multi-prototype alignment and routing to accurately associate queries with domain-specific knowledge bases.

**Neuron Attribution and DIF Embedding.** Using  $\mathcal{D}_{\text{probe}}$ , we estimate the importance of each neuron using Shapley-based attribution. For a transformer block at layer  $t$ , the feed-forward network (FFN) computes each neuron activation as:

$$\theta_{t,j} = \text{ACT}([h_t W_{t1} + b_{t1}]_j), \quad (3)$$

where  $h_t \in \mathbb{R}^d$  is the output of the attention sublayer,  $W_{t1} \in \mathbb{R}^{d \times 4d}$  and  $b_{t1} \in \mathbb{R}^{4d}$  are projection weights and biases, and  $\text{ACT}(\cdot)$  denotes the nonlinearity. For each parameter  $\theta_j \in \Theta$ , we approximate its Shapley value  $\phi_j$ :

$$\phi_j = -g_j^{(\gamma)} \theta_j - \frac{1}{2} \omega_{jj}^{(j)} \theta_j^2 H_{jj}^{(\gamma)} - \frac{1}{2} \theta_j \sum_{k \neq j} \omega_{jk}^{(S)} H_{jk}^{(\gamma)} \theta_k, \quad (4)$$

where  $g_j^{(\gamma)} = \partial \mathcal{L}_{\text{SFT}} / \partial \theta_j$  is the supervised loss gradient, and  $H_{jk}^{(\gamma)}$  is the Hessian capturing second-order interactions.

The coefficients  $\omega_{jj}^{(j)}$  and  $\omega_{jk}^{(S)}$  weight self and pairwise contributions, respectively.

We then: ❶. Select the top- $T$  layers based on aggregated Shapley scores. ❷. Within each selected layer, identify the most informative neuron groups (adjacent units with the highest  $\phi_j$ ). ❸. For a query  $x$ , concatenate the activations of these groups to form the DIF representation:

$$\mathbf{z} = \text{CONCAT}(\{h_{\ell_i}^{(g_i)}\}_{i=1}^P), \quad (5)$$

where  $\ell_i \in \mathcal{L}_{\text{top}}$  and  $g_i$  indexes the selected neuron groups. The resulting  $\mathbf{z}$  captures both semantic intent and domain cues, and serves as the input for for both inter- and intra-knowledge-base modeling. (Section 3.3).

### 3.3 Multi-Prototype Knowledge Alignment & Routing

To bridge internal DIF representations and external distributed knowledge structure (C2), we map  $\mathbf{z}$  to a semantic space using a projection  $g_{\text{align}}$ , producing  $\mathbf{r} = g_{\text{align}}(\mathbf{z})$ .

We train this space with two contrastive stages and use it for prototype-guided routing.

**Inter-KB Alignment.** We apply supervised contrastive learning to model the boundary between different knowledge bases:

$$\mathcal{L}_{\text{CL}} = - \sum_i \frac{1}{|P(i)|} \sum_{p \in P(i)} \log \frac{\exp(\mathbf{r}_i^\top \mathbf{r}_p / \tau_{cl})}{\sum_{a \in A(i)} \exp(\mathbf{r}_i^\top \mathbf{r}_a / \tau_{cl})}, \quad (6)$$

where  $P(i)$  denotes all in-batch positive samples that share the same knowledge base as  $i$ , excluding  $i$  itself, and  $A(i)$  includes all other in-batch samples except  $i$ .  $\tau \in \mathbb{R}^+$  is a scalar temperature parameter.

**Intra-KB Alignment.**

Besides inter-KB modeling, we perform intra-KB modeling to capture fine-grained variations. Specifically, we first cluster embeddings within each class into prototypes  $\{\mu_m\}_{m=1}^M$  using KMeans to obtain initial cluster centers, which are then used to initialize and optimize  $\mathcal{L}_{\text{PCL}}$  for more detailed fine-grained modeling:

$$\mathcal{L}_{\text{PCL}} = - \sum_i \frac{1}{|C(i)|} \sum_{m \in C(i)} \log \frac{\exp(\mathbf{r}_i^\top \mu_m / \tau_{pcl})}{\sum_{j \in AC(i)} \exp(\mathbf{r}_i^\top \mu_j / \tau_{pcl})}, \quad (7)$$

where  $C(i)$  denotes the set of prototypes most similar to  $\mathbf{r}_i$  based on cosine similarity (typically the nearest prototype), and  $AC(i)$  represents all prototypes excluding those in  $C(i)$ . During inference, given a query embedding  $\mathbf{q}$ , we compute its similarity scores  $s_i = \text{sim}(\mathbf{q}, \mu_i)$  to all learned prototypes  $\mu_i$ . The routing function then proceeds in two stages:

**Adaptive triggering.** If the maximum similarity falls below a threshold  $\tau$ , i.e.,  $\max_i s_i < \tau$ , the system abstains

from retrieval.

$$f_{\text{route}}(\mathbf{q}) = \begin{cases} \mathbf{0}, & \max_i s_i < \tau, \\ [w_1, \dots, w_K], & \text{otherwise} \end{cases} \quad (8)$$

**Semantic Routing.** Otherwise, it identifies the top- $N$  most similar prototypes  $\mathcal{I}$  and allocates a total of  $T$  retrieval slots across knowledge bases. The number of documents assigned to each knowledge base  $k$  is computed as:

$$w_k = \left\lfloor \frac{\sum_{i \in \mathcal{I}, k_i=k} s_i}{\sum_{k'} \sum_{i \in \mathcal{I}, k_i=k'} s_i} \cdot T \right\rfloor. \quad (9)$$

This two-step mechanism ensures that retrieval is triggered only when necessary and distributes resources based on prototype-level semantic relevance.

## 4 Experiments

We conduct extensive experiments across multiple datasets to evaluate the effectiveness of DFAMS in Federated Retrieval settings. Our experiment is organized to answer the following key research questions:

- **RQ1 (Section 4.2):** Does DFAMS consistently outperform existing advanced methods?
- **RQ2 (Section 4.3):** How do the proposed component contribute to the observed performance improvements?
- **RQ3 (Section 4.4):** How sensitive is DFAMS to variations in model configurations?

### 4.1 Experimental Setup

**LLM Backbones.** We implement DFAMS on four open-weight, decoder-only LLMs with varying scales to evaluate scalability and generalization: *Qwen2.5-0.5B*, *Qwen2.5-3B*, *Qwen2.5-7B* (Yang et al. 2024), and *Llama3.1-8B* (Grattafiori et al. 2024).

**Retrieval Configuration.** DFAMS utilizes FAISS (Douze et al. 2024) for dense vector retrieval across three federated retrieval (FR) scenarios, each comprising multiple knowledge bases: *Wiki-KB* (10 semantically clustered segments from Wikipedia (Wu et al. 2025)), *Med-KB* (4 sources: PubMed, StatPearls, textbooks, and medical Wikipedia (Zhao et al. 2025)), and *PEP-KB* (4 collections of internal enterprise policy documents). For each query, the top-10 chunks are retrieved collectively from the selected sources across all relevant knowledge bases within the same scenario. Further details on the retrieval pipeline and indexing strategies are provided in Appendix D.

**Datasets.** Based on the above knowledge base configurations, we construct three in-domain evaluation benchmarks—*Wiki*, *Med*, and *PEP*—each aligned with one of the FR scenarios and following the data setup described in Section 3.1. To further evaluate out-of-domain (OOD) generalization, we test models trained on Wiki and Med using a filtered subset of *MMLU* (Hendrycks et al. 2020) and a subset of *MIRAGE* (Xiong et al. 2024), respectively, with retrieval grounded in their corresponding knowledge bases. Further construction details are provided in Appendix E.

**Baselines.** We compare DFAMS with several representative retrieval and routing strategies: *No-RAG*, *Merged-RAG* (merges all corpora into one retrieval space), and two prompt-based methods—*Prompt* and *CoTPrompt* (Wei et al. 2023). We also include two recent multi-source retrieval approaches: *RAGRoute* (Guerraoui et al. 2025) that employs a binary classifier for each knowledge base to select the Top- $k$  sources, and *RopMura* (Wu et al. 2025), a prototype-based multi-agent routing method. Implementation details are provided in Appendix F.

**Evaluation Metrics.** We report three complementary metrics: (1) **Cls Acc**, which measures whether the predicted knowledge base(s) match the ground truth, including correct `Others` predictions for no-retrieval cases; (2) **Recall**, computed over Top-10 retrieved documents for retrieval-triggering queries, measuring the proportion of gold documents successfully retrieved excluding no-retrieval cases; (3) **QA**, the end-to-end answer accuracy, using accuracy(QA ACC) for multiple-choice and LLM-based scoring (QA Score) (Zheng et al. 2023) for open-ended questions. More metric details are available in Appendix G.

### 4.2 Main Result Analysis (RQ1)

To address *RQ1*, we train DFAMS on the *Wiki*, *Med*, and *PEP* datasets, and evaluate it on both in-domain (Wiki, Med, PEP) and out-of-domain (MMLU, MIRAGE) benchmarks using *Qwen2.5-7B* and *LLaMA3.1-8B*, comparing against baselines from retrieval, prompt-based, and multi-source routing methods.

**Comparison with Baselines.** Table 1 summarizes the performance of DFAMS compared with a range of baseline methods across three key metrics: Cls Acc, Recall, and QA Acc/Score. DFAMS consistently outperforms all baselines on both in-domain and out-of-domain (OOD) datasets.

**Comparison of Advanced Multi-Source Retrieval and Naive Methods.** In most cases, multi-source retrieval methods (*RopMura*, *RAGRoute*) achieve higher CLS ACC and Recall than *Prompt*-based or *Merged-RAG* baselines in most cases. For example, on the Wiki dataset with *Qwen2.5-7B*, *RAGRoute* achieves a Cls Acc of 76.07% and recall of 50.04%, compared to just 32.47% and 25.93% from *Prompt*. Similarly, *RopMura* outperforms *Merged-RAG* on Med in Recall (41.59% vs. 33.89%). While multi-source retrieval methods (*RopMura*, *RAGRoute*) generally achieve higher recall through broader source coverage, these gains often come at the cost of increased cross-domain noise. For instance, although *RAGRoute* obtains higher recall on the Med dataset, its QA accuracy (73.64%) falls short of that of *Merged-RAG* (79.60%). In contrast, prompt-based methods adopt a more conservative source selection strategy, often retrieving from fewer knowledge bases, which helps reduce cross-domain noise. Merged methods, on the other hand, rely on dense semantic similarity across the entire corpus; while the retrieved chunks may not always be precisely grounded, they tend to be semantically coherent.

**Comparison of DFAMS and Advanced Multi-Source Retrieval.** Compared with advanced multi-source retrieval

Method	In-Domain								Out-of-Domain	
	Wiki			Med			PEP		MMLU	MIRAGE
	Cls Acc (↑)	Recall (↑)	QA Acc (↑)	Cls Acc (↑)	Recall (↑)	QA Acc (↑)	Cls Acc (↑)	QA Score (↑)	QA Acc (↑)	QA Acc (↑)
<i>Qwen2.5-7B</i>										
No RAG	/	/	59.30	/	/	75.20	/	7.56	79.05	68.05
Merged-RAG	/	48.49	77.20	/	33.89	79.60	/	8.33	77.74	65.78
Prompt	32.47	25.93	63.66	48.82	34.68	79.59	66.86	6.21	80.77	69.17
COT Prompt	58.67	38.17	71.40	48.82	31.40	80.72	77.91	5.92	80.52	69.47
RopMura	62.83	48.92	77.47	53.09	41.59	82.01	75.92	7.18	80.38	69.97
RAGRoute	76.07	50.04	78.40	69.04	35.78	73.64	51.47	7.14	80.20	69.77
<b>DFAMS</b>	<b>85.03</b>	<b>53.83</b>	<b>78.94</b>	<b>71.81</b>	<b>42.82</b>	<b>82.82</b>	<b>82.85</b>	<b>8.39</b>	<b>86.17</b>	<b>79.88</b>
<i>LLaMA3.1-8B</i>										
No RAG	/	/	60.40	/	/	68.27	/	5.35	59.31	61.90
Merged-RAG	/	48.49	76.48	/	33.89	74.17	/	5.38	56.30	62.68
Prompt	36.18	25.93	64.67	49.57	34.72	71.65	65.99	5.17	63.90	61.51
COT Prompt	58.20	38.14	68.98	48.92	31.59	74.46	76.75	4.82	63.55	63.43
RopMura	62.83	48.92	76.78	53.09	41.59	75.37	75.92	4.46	64.06	61.82
RAGRoute	76.07	50.04	76.83	69.04	35.78	74.55	51.47	4.58	64.37	63.16
<b>DFAMS</b>	<b>84.36</b>	<b>53.83</b>	<b>78.60</b>	<b>72.57</b>	<b>42.82</b>	<b>77.65</b>	<b>81.98</b>	<b>8.08</b>	<b>64.89</b>	<b>64.89</b>

Table 1: Performance comparison (%) on *Wiki*, *Med*, *PEP*, *MMLU*, and *MIRAGE*, where **bold** indicates the best result, and symbol slash “/” denotes inapplicable metrics due to lack of retrieval (NoRAG) or single-source setup (Merged RAG).

methods, DFAMS consistently achieves higher CLS ACC and Recall across all datasets and model backbones. For instance, on Wiki with Qwen2.5-7B, DFAMS outperforms RAGRoute by +8.96% in CLS Acc (85.03% vs. 76.07%) and +3.79% in Recall (53.83% vs. 50.04%). These improvements stem from DFAMS’s fine-grained modeling of FID, enabling more accurate identification of query intent and relevant knowledge sources. This leads to better routing and more focused retrieval with less cross-domain noise. As a result, DFAMS consistently achieves the highest QA accuracy across all datasets. For example, on the Qwen2.5-7B backbone, it reaches 82.82% QA accuracy on Med and 78.94% on Wiki, outperforming both RopMura and RAGRoute.

**Adaptive Retrieval Capability.** DFAMS learns to decide whether external retrieval is needed for a given query. We evaluate its adaptive retrieval capability by grouping all sources into a single Knowledge class and using an Others class for queries answerable via parametric knowledge. As shown in Table 2, DFAMS achieves high accuracy on Wiki (99.95%) and Med (93.67%), closely matching *Probing RAG* and significantly outperforming the *Prompt*-based approach. These results highlight DFAMS’s ability to avoid unnecessary retrieval while preserving high coverage when external information is required.

Method	Wiki Acc (↑)	Med Acc (↑)
Prompt	69.73	84.20
Probing RAG	<b>99.98</b>	92.80
<b>DFAMS</b>	99.95	<b>93.67</b>

Table 2: Adaptive retrieval accuracy comparison between different methods on Wiki and Med datasets.

**Inference Efficiency.** We assess DFAMS’s efficiency by measuring average routing, retrieval, and total latency per sample on the Med dataset (Table 3). Despite relying on LLMs, DFAMS achieves a low end-to-end latency of 1.48s—substantially faster than *Prompt* (15.59s) and *Merged-RAG* (3.89s). Compared to *RAGRoute* (1.64s), DFAMS is slightly faster due to retrieving from fewer sources. In RAGRoute, its pursuit of higher recall often triggers more knowledge bases, and slower sources can increase latency despite parallel execution. Overall, DFAMS offers faster inference with precise routing.

Method	Routing (s)	Retrieval (s)	Total (s)
Prompt	14.25	1.35	15.59
Merged-RAG	<b>0</b>	3.89	3.89
RAGRoute	0.0023	1.64	1.64
<b>DFAMS</b>	0.13	<b>1.34</b>	<b>1.48</b>

Table 3: Comparison of routing, retrieval, and total processing times for different methods on the Med dataset.

### 4.3 Ablation Study (RQ2)

To answer **RQ2**, we conduct ablation studies on the two core components of DFAMS: (1) *Dynamic Information Flow Modeling* and (2) *Multi-Prototype Knowledge Alignment and Routing*, aiming to investigate their individual contributions to the overall system performance.

**Dynamic Information Flow Modeling.** We conduct ablation studies to test our central hypothesis: that DIF signals not only exist but can be effectively detected and exploited to improve model performance. We design two experimental settings: (1) Frozen LLM w/o Align-MLP: We remove the trainable Align-MLP and directly utilize

the extracted FID. This setting investigates whether native LLM activations inherently encode subdomain-aware signals—i.e., whether meaningful associations between user queries and knowledge subdomains can be inferred without explicit alignment. (2) Full DFAMS (w/ Align-MLP): We enable the trainable Align-MLP to utilize DIF to assess whether modeling the knowledge base on FID leads to improved alignment and enhanced downstream performance.

Method	Wiki ( $\uparrow$ )	Med ( $\uparrow$ )
<i>Frozen (no Align-MLP)</i>		
Random	53.19	42.90
Full	62.67	53.29
<b>DFAMS</b>	<b>67.74</b>	<b>54.68</b>
<i>Trained (with Align-MLP)</i>		
Random	81.49	66.47
Full	83.37	69.65
<b>DFAMS</b>	<b>85.03</b>	<b>71.81</b>

Table 4: Ablation analysis of Dynamic Information Flow modeling on Wiki and Med datasets

We conduct experiments on both the *Wiki* and *Med* datasets. Table 4 shows that in setting (1), DFAMS (2000-dim) outperforms both random (2000-dim) and full-layer (3584-dim) baselines, achieving +14.6% accuracy gain on Wiki and +11.78% on Med over the random baseline. These results validate our hypothesis: FID captures query-subdomain associations and can be directly leveraged, even without further training. In setting (2), with Align-MLP enabled, DFAMS achieves +3.54% and +1.66% higher accuracy than the random and full-layer baselines on Wiki, and +5.34% and +2.16% on Med, respectively. These results highlight the benefit of leveraging DIF for knowledge base modeling, resulting in better alignment and improved downstream performance. Additional results and analyses are provided in Appendix D.

Variant	Accuracy ( $\uparrow$ )	Recall ( $\uparrow$ )
<b>Full Method</b>	<b>85.03</b>	<b>53.83</b>
<i>w/o Inter-KB Alignment</i>	75.89	52.09
<i>w/o Intra-KB Alignment</i>	83.28	50.68
<i>w/o Adaptive Triggering</i>	79.56	<b>53.83</b>
<i>w/o Semantic Routing</i>	80.67	48.67

Table 5: Ablation Analysis of Multi-Prototype Alignment and Routing Components on Wiki dataset

**Ablation on Multi-Prototype Knowledge Alignment and Routing** We conduct targeted ablations to evaluate the impact of DFAMS’s core components. Results are shown in Table 5. Disabling inter-KB alignment, which separates semantic boundaries across knowledge bases, causes the CIs ACC drop (-9.14%), highlighting its key role in knowledge base selection and adaptive retrieval. Removing intra-KB alignment, responsible for modeling knowledge bases’

subdomain structures via multi-prototype contrastive learning, leads to the biggest recall decline (-3.15%), showing its importance for accuracy and high quality retrieval. On the inference side, removing adaptive triggering reduces accuracy (-5.47%), as the model can no longer skip unnecessary retrieval. Disabling Semantic Routing, which confines retrieval to only one top source, further decreases recall (-5.16%), highlighting the value of semantic-aware resource allocation across multiple knowledge bases.

#### 4.4 Sensitivity Analysis (RQ3)

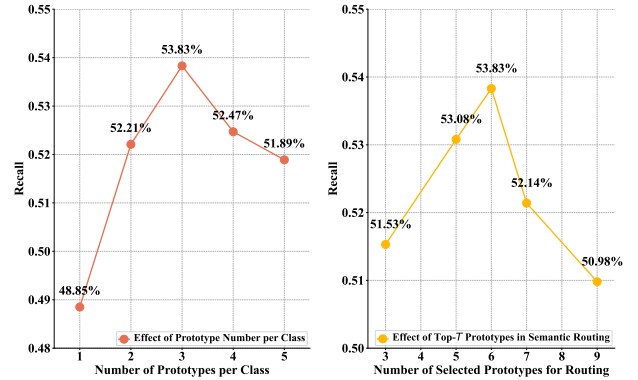


Figure 3: Hyperparameter Analysis of Prototypes per Class (Left) and Selected Prototypes for Routing (Right)

To assess how sensitive DFAMS is to variations in key configurations, we conduct experiments on the Wiki dataset.

**Effect of Prototype Number.** From the result in Figure 3 (left), the accuracy increases with prototype count, peaking at 3 (53.8%), then declines (e.g., 52.1% at 4), suggesting that too few prototypes underfit subdomain diversity, while too many cause over-fragmentation.

**Effect of Semantic Routing Top- $T$ .** As shown in Figure 3 (right), when top- $T$  is 3, it achieves the best balance (84.2% accuracy, 53.8% recall). Lower  $T$  values miss relevant sources, while higher  $T$  dilutes document allocation across knowledge bases, reducing the chance of retrieving key information.

## 5 Conclusions and Future Works

We propose DFAMS, a novel FR framework that explicitly models the DIF within LLMs to enhance query understanding and cross-source knowledge alignment. By leveraging gradient-based neuron attribution and Shapley value estimation, DFAMS identifies latent neural activation paths that reflect user intent and subdomain relevance. The framework also introduces a Multi-Prototype Knowledge Alignment and Routing strategy, which enables fine-grained modeling of individual knowledge bases, effectively preserving inter-source semantic associations while supporting multi-knowledge-base routing. Our experiments show that DFAMS consistently outperforms existing FR baselines in

knowledge base classification, retrieval quality, and end-to-end QA performance, confirming its effectiveness in resolving semantic ambiguities and improving cross-source routing in complex settings.

Future efforts will focus on optimizing prototype selection and update strategies, integrating DFAMS with advanced RAG techniques for improved end-to-end reasoning, and exploring its applicability in other specialized domains such as legal, finance, and scientific research.

## References

- Adamczewski, K.; Li, Y.; and van Gool, L. 2024. Shapley Pruning for Neural Network Compression. *arXiv:2407.15875*.
- Addison, P.; Nguyen, M.-T. H.; Medan, T.; Shah, J.; Manzari, M. T.; McElrone, B.; Lalwani, L.; More, A.; Sharma, S.; Roth, H. R.; et al. 2024. C-fedrag: A confidential federated retrieval-augmented generation system. *arXiv preprint arXiv:2412.13163*.
- Arbib, M. A. 2003. *The handbook of brain theory and neural networks*. MIT press.
- Asai, A.; Min, S.; Zhong, Z.; and Chen, D. 2023. Retrieval-based language models and applications. In *Proceedings of the 61st Annual Meeting of the Association for Computational Linguistics (Volume 6: Tutorial Abstracts)*, 41–46.
- Asai, A.; Wu, Z.; Wang, Y.; Sil, A.; and Hajishirzi, H. 2024. Self-RAG: Learning to Retrieve, Generate, and Critique through Self-Reflection. In *ICLR*.
- Baek, I.; Chang, H.; Kim, B.; Lee, J.; and Lee, H. 2025. Probing-RAG: Self-Probing to Guide Language Models in Selective Document Retrieval. In *Findings of the Association for Computational Linguistics: NAACL 2025*, 3287–3304.
- Bai, J.; Bai, S.; Chu, Y.; Cui, Z.; Dang, K.; Deng, X.; Fan, Y.; Ge, W.; Han, Y.; Huang, F.; et al. 2023. Qwen technical report. *arXiv preprint arXiv:2309.16609*.
- Bandarkar, L.; Muller, B.; Yuvraj, P.; Hou, R.; Singhal, N.; Lv, H.; and Liu, B. 2024. Layer swapping for zero-shot cross-lingual transfer in large language models. *arXiv preprint arXiv:2410.01335*.
- Bhavnani, S. K.; and Wilson, C. S. 2009. Information scattering. *Encyclopedia of library and information sciences*, 2564–2569.
- Cao, M.; Dong, Y.; Wu, J.; and Cheung, J. C. K. 2020. Factual Error Correction for Abstractive Summarization Models. In *Proceedings of the 2020 Conference on Empirical Methods in Natural Language Processing (EMNLP)*, 6251–6258. Online: Association for Computational Linguistics.
- Chakraborty, A.; Dahal, C.; and Gupta, V. 2025. Federated Retrieval-Augmented Generation: A Systematic Mapping Study. *arXiv preprint arXiv:2505.18906*.
- Clarke, C. L.; Kolla, M.; Cormack, G. V.; Vechtomova, O.; Ashkan, A.; Büttcher, S.; and MacKinnon, I. 2008. Novelty and diversity in information retrieval evaluation. In *Proceedings of the 31st annual international ACM SIGIR conference on Research and development in information retrieval*, 659–666.
- Dai, D.; Dong, L.; Hao, Y.; Sui, Z.; Chang, B.; and Wei, F. 2021. Knowledge neurons in pretrained transformers. *arXiv preprint arXiv:2104.08696*.
- Dhamdhere, K.; Sundararajan, M.; and Yan, Q. 2018. How important is a neuron? *arXiv preprint arXiv:1805.12233*.
- Douze, M.; Guzhva, A.; Deng, C.; Johnson, J.; Szilvassy, G.; Mazaré, P.-E.; Lomeli, M.; Hosseini, L.; and Jégou, H. 2024. The Faiss library.
- Edge, D.; Trinh, H.; Cheng, N.; Bradley, J.; Chao, A.; Mody, A.; Truitt, S.; and Larson, J. 2024. From Local to Global: A Graph RAG Approach to Query-Focused Summarization. *arXiv:2404.16130*.
- Feng, Y.; Chu, X.; Xu, Y.; Shi, G.; Liu, B.; and Wu, X.-M. 2024. Tasl: Continual dialog state tracking via task skill localization and consolidation. *arXiv preprint arXiv:2408.09857*.
- Feng, Y.; Wang, X.; Lu, Z.; Fu, S.; Shi, G.; Xu, Y.; Wang, Y.; Yu, P. S.; Chu, X.; and Wu, X.-M. 2025. Recurrent Knowledge Identification and Fusion for Language Model Continual Learning. *arXiv:2502.17510*.
- Gao, L.; Ma, X.; Lin, J.; and Callan, J. 2022. Precise Zero-Shot Dense Retrieval without Relevance Labels. *arXiv:2212.10496*.
- Ghorbani, A.; and Zou, J. Y. 2020. Neuron shapley: Discovering the responsible neurons. *Advances in neural information processing systems*, 33: 5922–5932.
- Grattafiori, A.; Dubey, A.; Jauhri, A.; Pandey, A.; Kadian, A.; Al-Dahle, A.; Letman, A.; Mathur, A.; Schelten, A.; Vaughan, A.; et al. 2024. The llama 3 herd of models. *arXiv preprint arXiv:2407.21783*.
- Guerraoui, R.; Kermarrec, A.-M.; Petrescu, D.; Pires, R.; Randl, M.; and de Vos, M. 2025. Efficient federated search for retrieval-augmented generation. In *Proceedings of the 5th Workshop on Machine Learning and Systems*, 74–81.
- Hawrylycz, M. J.; Lein, E. S.; Guillozet-Bongaarts, A. L.; Shen, E. H.; Ng, L.; Miller, J. A.; Van De Lagemaat, L. N.; Smith, K. A.; Ebbert, A.; Riley, Z. L.; et al. 2012. An anatomically comprehensive atlas of the adult human brain transcriptome. *Nature*, 489(7416): 391–399.
- Hendrycks, D.; Burns, C.; Basart, S.; Zou, A.; Mazeika, M.; Song, D.; and Steinhardt, J. 2020. Measuring massive multitask language understanding. *arXiv preprint arXiv:2009.03300*.
- Huang, C.; Dong, X.; Li, Z.; Song, T.; Liu, Z.; and Dong, L. 2021. Efficient Stride 2 Winograd Convolution Method Using Unified Transformation Matrices on FPGA. In *2021 International Conference on Field-Programmable Technology (ICFPT)*, 1–9. IEEE.
- Huang, Y.; and Huang, J. 2024. A survey on retrieval-augmented text generation for large language models. *arXiv preprint arXiv:2404.10981*.
- Huo, J.; Yan, Y.; Hu, B.; Yue, Y.; and Hu, X. 2024. Mm-neuron: Discovering neuron-level domain-specific interpretation in multimodal large language model. *arXiv preprint arXiv:2406.11193*.

- Jeon, B.; Ferdous, S.; Rahman, M. R.; and Walid, A. 2021. Privacy-preserving decentralized aggregation for federated learning. In *IEEE INFOCOM 2021-IEEE Conference on Computer Communications Workshops (INFOCOM WKSHPS)*, 1–6. IEEE.
- Jeong, S.; Baek, J.; Cho, S.; Hwang, S. J.; and Park, J. C. 2024. Adaptive-rag: Learning to adapt retrieval-augmented large language models through question complexity. *arXiv preprint arXiv:2403.14403*.
- Ji, Z.; Lee, N.; Frieske, R.; Yu, T.; Su, D.; Xu, Y.; Ishii, E.; Bang, Y. J.; Madotto, A.; and Fung, P. 2023. Survey of Hallucination in Natural Language Generation. *ACM Comput. Surv.*, 55(12).
- Jiang, E. 2024. *Clinical question-answering over distributed EHR data*. Ph.D. thesis, Massachusetts Institute of Technology.
- Jiang, G.; Jiang, C.; Li, Z.; Xue, S.; Zhou, J.; Song, L.; Lian, D.; and Wei, Y. 2025. Unlocking the Power of Function Vectors for Characterizing and Mitigating Catastrophic Forgetting in Continual Instruction Tuning. *arXiv:2502.11019*.
- Jiang, X.; Fang, Y.; Qiu, R.; Zhang, H.; Xu, Y.; Chen, H.; Zhang, W.; Zhang, R.; Chu, X.; Zhao, J.; et al. 2024a. TC-RAG: Turing-Complete RAG’s Case study on Medical LLM Systems. *CoRR*.
- Jiang, X.; Zhang, R.; Xu, Y.; Qiu, R.; Fang, Y.; Wang, Z.; Tang, J.; Ding, H.; Chu, X.; Zhao, J.; and Wang, Y. 2024b. HyKGE: A Hypothesis Knowledge Graph Enhanced Framework for Accurate and Reliable Medical LLMs Responses. *arXiv:2312.15883*.
- Jung, J.; Jeong, H.; and Huh, E.-N. 2025. Federated learning and RAG integration: a scalable approach for medical large language models. In *2025 International Conference on Artificial Intelligence in Information and Communication (ICAIIIC)*, 0968–0973. IEEE.
- Kairouz, P.; McMahan, H. B.; Avent, B.; Bellet, A.; Bennis, M.; Bhagoji, A. N.; Bonawitz, K.; Charles, Z.; Cormode, G.; Cummings, R.; et al. 2021. Advances and open problems in federated learning. *Foundations and trends® in machine learning*, 14(1–2): 1–210.
- Kaplan, J.; McCandlish, S.; Henighan, T.; Brown, T. B.; Chess, B.; Child, R.; Gray, S.; Radford, A.; Wu, J.; and Amodei, D. 2020. Scaling Laws for Neural Language Models. *arXiv:2001.08361*.
- Kukreja, S.; Kumar, T.; Bharate, V.; Purohit, A.; Dasgupta, A.; and Guha, D. 2024. Performance evaluation of vector embeddings with retrieval-augmented generation. In *2024 9th International Conference on Computer and Communication Systems (ICCCS)*, 333–340. IEEE.
- LeCun, Y.; Denker, J.; and Solla, S. 1989. Optimal brain damage. *Advances in neural information processing systems*, 2.
- Lewis, P.; Perez, E.; Piktus, A.; Petroni, F.; Karpukhin, V.; Goyal, N.; Küttler, H.; Lewis, M.; Yih, W.-t.; Rocktäschel, T.; et al. 2020. Retrieval-augmented generation for knowledge-intensive nlp tasks. *Advances in Neural Information Processing Systems*, 33: 9459–9474.
- Li, Z.; Zhang, X.; Zhang, Y.; Long, D.; Xie, P.; and Zhang, M. 2023. Towards general text embeddings with multi-stage contrastive learning. *arXiv preprint arXiv:2308.03281*.
- Liang, S.; Sun, H.; Lin, T.-E.; Wu, Y.; Wang, Z.; Li, Y.; and Yan, R. 2024. Locate-then-Unlearn: An Effective Method of Multi-Task Continuous Learning for Large Language Models.
- OpenAI. 2022. Introducing ChatGPT. <https://openai.com/blog/chatgpt>.
- OpenAI. 2023. GPT-4 Technical Report. *ArXiv*, abs/2303.08774.
- Peng, H.; Li, H.; Song, Y.; Zheng, V.; and Li, J. 2021. Differentially private federated knowledge graphs embedding. In *Proceedings of the 30th ACM international conference on information & knowledge management*, 1416–1425.
- Ryan, M. J.; Xu, D.; Nivera, C.; and Campos, D. 2025. Enronqa: Towards personalized rag over private documents. *arXiv preprint arXiv:2505.00263*.
- Schölkopf, B. 2019. Causality for Machine Learning. 1–20.
- Shojaee, P.; Harsha, S. S.; Luo, D.; Maharaj, A.; Yu, T.; and Li, Y. 2025. Federated retrieval augmented generation for multi-product question answering. *arXiv preprint arXiv:2501.14998*.
- Shokouhi, M.; Si, L.; et al. 2011. Federated search. *Foundations and trends® in information retrieval*, 5(1): 1–102.
- Stolfo, A.; Belinkov, Y.; and Sachan, M. 2023. A Mechanistic Interpretation of Arithmetic Reasoning in Language Models using Causal Mediation Analysis. In *The 2023 Conference on Empirical Methods in Natural Language Processing*.
- Su, W.; Tang, Y.; Ai, Q.; Wu, Z.; and Liu, Y. 2024. Dragon: Dynamic retrieval augmented generation based on the real-time information needs of large language models. *arXiv preprint arXiv:2403.10081*.
- Sun, Q.; Pickett, M.; Nain, A. K.; and Jones, L. 2025. Transformer layers as painters. In *Proceedings of the AAAI Conference on Artificial Intelligence*, volume 39, 25219–25227.
- Tang, T.; Luo, W.; Huang, H.; Zhang, D.; Wang, X.; Zhao, X.; Wei, F.; and Wen, J.-R. 2024. Language-Specific Neurons: The Key to Multilingual Capabilities in Large Language Models. In Ku, L.-W.; Martins, A.; and Srikumar, V., eds., *Proceedings of the 62nd Annual Meeting of the Association for Computational Linguistics (Volume 1: Long Papers)*, 5701–5715. Bangkok, Thailand: Association for Computational Linguistics.
- Todd, E.; Li, M. L.; Sharma, A. S.; Mueller, A.; Wallace, B. C.; and Bau, D. 2023. Function vectors in large language models. *arXiv preprint arXiv:2310.15213*.
- Vu, M. D.; Wang, H.; Li, Z.; Chen, J.; Zhao, S.; Xing, Z.; and Chen, C. 2024. GPTVoiceTasker: LLM-Powered Virtual Assistant for Smartphone. *arXiv:2401.14268*.
- Wang, H.; Huang, W.; Deng, Y.; Wang, R.; Wang, Z.; Wang, Y.; Mi, F.; Pan, J. Z.; and Wong, K.-F. 2024a. Unims-rag: A unified multi-source retrieval-augmented generation for personalized dialogue systems. *arXiv preprint arXiv:2401.13256*.

- Wang, M.; Yao, Y.; Xu, Z.; Qiao, S.; Deng, S.; Wang, P.; Chen, X.; Gu, J.-C.; Jiang, Y.; Xie, P.; et al. 2024b. Knowledge mechanisms in large language models: A survey and perspective. *arXiv preprint arXiv:2407.15017*.
- Wang, S.; Khramtsova, E.; Zhuang, S.; and Zuccon, G. 2024c. Feb4rag: Evaluating federated search in the context of retrieval augmented generation. In *Proceedings of the 47th International ACM SIGIR Conference on Research and Development in Information Retrieval*, 763–773.
- Wang, W.; Bao, H.; Huang, S.; Dong, L.; and Wei, F. 2020. Minilmv2: Multi-head self-attention relation distillation for compressing pretrained transformers. *arXiv preprint arXiv:2012.15828*.
- Wang, Y.; Chen, Y.; Wen, W.; Sheng, Y.; Li, L.; and Zeng, D. D. 2024d. Unveiling factual recall behaviors of large language models through knowledge neurons. *arXiv preprint arXiv:2408.03247*.
- Wei, J.; Wang, X.; Schuurmans, D.; Bosma, M.; Ichter, B.; Xia, F.; Chi, E.; Le, Q.; and Zhou, D. 2023. Chain-of-Thought Prompting Elicits Reasoning in Large Language Models. *arXiv:2201.11903*.
- Wei, J.; Wang, X.; Schuurmans, D.; Bosma, M.; Xia, F.; Chi, E.; Le, Q. V.; Zhou, D.; et al. 2022. Chain-of-thought prompting elicits reasoning in large language models. *Advances in neural information processing systems*, 35: 24824–24837.
- Wendler, C.; Veselovsky, V.; Monea, G.; and West, R. 2024. Do llamas work in english? on the latent language of multilingual transformers. In *Proceedings of the 62nd Annual Meeting of the Association for Computational Linguistics (Volume 1: Long Papers)*, 15366–15394.
- Wu, F.; Li, Z.; Wei, F.; Li, Y.; Ding, B.; and Gao, J. 2025. Talk to right specialists: Routing and planning in multi-agent system for question answering. *arXiv preprint arXiv:2501.07813*.
- Wu, W.; Wang, Y.; Xiao, G.; Peng, H.; and Fu, Y. 2024. Retrieval head mechanistically explains long-context factuality. *arXiv preprint arXiv:2404.15574*.
- Xiong, G.; Jin, Q.; Lu, Z.; and Zhang, A. 2024. Benchmarking retrieval-augmented generation for medicine. In *Findings of the Association for Computational Linguistics ACL 2024*, 6233–6251.
- Xu, R.; Baracaldo, N.; Zhou, Y.; Anwar, A.; Kadhe, S.; and Ludwig, H. 2022. Detrust-fl: Privacy-preserving federated learning in decentralized trust setting. In *2022 IEEE 15th International Conference on Cloud Computing (CLOUD)*, 417–426. IEEE.
- Xu, Y.; Zhang, R.; Jiang, X.; Feng, Y.; Xiao, Y.; Ma, X.; Zhu, R.; Chu, X.; Zhao, J.; and Wang, Y. 2024. Parenting: Optimizing knowledge selection of retrieval-augmented language models with parameter decoupling and tailored tuning. *arXiv preprint arXiv:2410.10360*.
- Yang, A.; Yang, B.; Zhang, B.; Hui, B.; Zheng, B.; Yu, B.; Li, C.; Liu, D.; Huang, F.; Wei, H.; Lin, H.; Yang, J.; Tu, J.; Zhang, J.; Yang, J.; Yang, J.; Zhou, J.; Lin, J.; Dang, K.; Lu, K.; Bao, K.; Yang, K.; Yu, L.; Li, M.; Xue, M.; Zhang, P.; Zhu, Q.; Men, R.; Lin, R.; Li, T.; Xia, T.; Ren, X.; Ren, X.; Fan, Y.; Su, Y.; Zhang, Y.; Wan, Y.; Liu, Y.; Cui, Z.; Zhang, Z.; and Qiu, Z. 2024. Qwen2.5 Technical Report. *CoRR*, abs/2412.15115.
- Yin, K.; and Steinhardt, J. 2025. Which Attention Heads Matter for In-Context Learning? *arXiv preprint arXiv:2502.14010*.
- Yu, R.; Li, A.; Chen, C.-F.; Lai, J.-H.; Morariu, V. I.; Han, X.; Gao, M.; Lin, C.-Y.; and Davis, L. S. 2018. Nisp: Pruning networks using neuron importance score propagation. In *Proceedings of the IEEE conference on computer vision and pattern recognition*, 9194–9203.
- Yu, Z.; and Ananiadou, S. 2024. Interpreting Arithmetic Mechanism in Large Language Models through Comparative Neuron Analysis. In *Proceedings of the 2024 Conference on Empirical Methods in Natural Language Processing*, 3293–3306.
- Yuan, H.; Zhou, S.; and Yu, S. 2023. EHRDiff: Exploring Realistic EHR Synthesis with Diffusion Models. *arXiv:2303.05656*.
- Yuan, Y.; Abbasiantaeb, Z.; Aliannejadi, M.; and Deng, Y. 2025. Query Understanding in LLM-based Conversational Information Seeking. In *Proceedings of the 48th International ACM SIGIR Conference on Research and Development in Information Retrieval*, 4098–4101.
- Zador, A. M. 2019. A critique of pure learning and what artificial neural networks can learn from animal brains. *Nature communications*, 10(1): 3770.
- Zeng, H.; Yue, Z.; Jiang, Q.; and Wang, D. 2024. Federated recommendation via hybrid retrieval augmented generation. In *2024 IEEE International Conference on Big Data (Big-Data)*, 8078–8087. IEEE.
- Zhang, C.; Xie, Y.; Bai, H.; Yu, B.; Li, W.; and Gao, Y. 2021. A survey on federated learning. *Knowledge-Based Systems*, 216: 106775.
- Zhang, Q.; Chen, M.; Bukharin, A.; Karampatziakis, N.; He, P.; Cheng, Y.; Chen, W.; and Zhao, T. 2023. Adalora: Adaptive budget allocation for parameter-efficient fine-tuning. *arXiv preprint arXiv:2303.10512*.
- Zhao, D. 2024. Frag: Toward federated vector database management for collaborative and secure retrieval-augmented generation. *arXiv preprint arXiv:2410.13272*.
- Zhao, X.; Liu, S.; Yang, S.-Y.; and Miao, C. 2025. MedRAG: Enhancing Retrieval-augmented Generation with Knowledge Graph-Elicited Reasoning for Healthcare Copilot. In *Proceedings of the ACM on Web Conference 2025*, 4442–4457.
- Zheng, L.; Chiang, W.-L.; Sheng, Y.; Zhuang, S.; Wu, Z.; Zhuang, Y.; Lin, Z.; Li, Z.; Li, D.; Xing, E. P.; Zhang, H.; Gonzalez, J. E.; and Stoica, I. 2023. Judging LLM-as-a-judge with MT-Bench and Chatbot Arena. *arXiv:2306.05685*.
- Zheng, Z.; Wang, Y.; Huang, Y.; Song, S.; Yang, M.; Tang, B.; Xiong, F.; and Li, Z. ????. Attention heads of large language models: A survey. *arXiv 2024. arXiv preprint arXiv:2409.03752*.

Zheng, Z.; Wang, Y.; Huang, Y.; Song, S.; Yang, M.; Tang, B.; Xiong, F.; and Li, Z. 2024. Attention heads of large language models: A survey. *arXiv preprint arXiv:2409.03752*.

## Appendix

### A. Notations Table

This section presents a comprehensive list of key notations and symbols employed in the DFAMS framework.

Symbol	Description
$I$	Number of isolated knowledge bases (KBs)
$\mathcal{K}_i = \{d_{i\ell}\}_{\ell=1}^{M_i}$	The $i$ -th KB containing $M_i$ documents $d_{i\ell}$
$x$	Input query for KBs selection and retrieval
$f_{\text{route}}$	Maps $x$ to document allocations over KBs
$\mathbf{w} = [w_1, \dots, w_I]$	Document allocation vector; $w_j$ is the number retrieved from $\mathcal{K}_j$
$\Theta$	Parameterized knowledge in the LLM
$\mathcal{D} = \mathcal{K}_1, \dots, \mathcal{K}_I$	KBs representing non-parameterized knowledge
$R$	Retrieved subset of KBs for answering the query
$\mathcal{P}$	Task-specific prompt
$y$	Ground-truth answer (or response) to query $x$
$\mathcal{D}_{\text{probe}}$	Dedicated probing dataset for neuron attribution and domain selection analysis
$h_t$	Output of attention sublayer in layer $t$
$W_{t1}, b_{t1}$	FFN projection weights and biases at layer $t$
$\text{ACT}(\cdot)$	Activation function
$\phi_j$	Shapley value for neuron $j$
$g_j^{(\gamma)}$	Gradient of supervised loss w.r.t. $\theta_j$
$H_{jk}^{(\gamma)}$	Hessian of loss capturing 2nd-order interactions
$\omega_{jj}^{(j)}$	Weighting coefficient for self-contribution of neuron $j$ in Shapley approximation
$\omega_{jk}^{(S)}$	Weighting coefficient for pairwise contribution between neurons $j$ and $k$
$\mathbf{z}$	DIF embedding composed of high-attribution neuron activations
$\text{CONCAT}(\cdot)$	Concatenates input set into a single vector
$g_{\text{align}}$	Projection function (Align MLP) mapping $\mathbf{z}$ to aligned query embedding $\mathbf{r}$ in the semantic space
$\mathcal{L}_{\text{CL}}$	supervised contrastive loss
$B$	Batch size used for contrastive training
$P(i)$	Set of in-batch positive samples sharing the same KB label as sample $i$
$A(i)$	All other in-batch samples excluding $i$ (i.e., positive + negative candidates)
$\tau_{\text{cl}}$	Temperature scaling factor in contrastive loss
$\mu_m$	Prototype vector in the contrastive-aligned space
$\mathcal{L}_{\text{PCL}}$	Intra-KB prototype contrastive loss
$C(i)$	Closest prototype(s) to sample $i$
$AC(i)$	All prototypes excluding those in $C(i)$
$\mathbf{q}$	Embedded representation of an unseen query
$\tau_{\text{pcl}}$	Temperature scaling factor in $\mathcal{L}_{\text{PCL}}$
$\text{sim}(\cdot, \cdot)$	Cosine similarity between two embeddings
$s_i$	Similarity between $\mathbf{q}$ and prototype $\mathbf{p}_i$
$T$	Total retrieval slots to be allocated
$\tau$	Adaptive triggering threshold
$\mathcal{I}$	Top- $N$ nearest prototypes

Table 6: Key Notations used in the DFAMS framework

### B. Algorithm

In this section, we detail the full DFAMS workflow, spanning its probing, training, and inference stages. Algorithm 1 identifies domain-sensitive neurons in pretrained LLMs, while Algorithm 2 describes the training procedure. Finally, Algorithm 3 presents the adaptive prototype-guided routing mechanism used during inference to dynamically allocate retrieval resources based on semantic relevance.

#### Algorithm 1: Neuron Probing for DIF Extraction

**Require:** Probing dataset  $\mathcal{D}_{\text{probe}} = \{(x_i, \mathcal{K}_i)\}$ , pretrained LLM  $\Theta$ , layer count  $L$ , top layer number  $T$ , neuron group size  $G$

**Ensure:** DIF-relevant neuron set  $\mathcal{N}$

- 1: Initialize Shapley values  $\Phi \leftarrow \mathbf{0}$  for all neurons in  $\Theta$
- 2: **for**  $(x_i, \mathcal{K}_i) \in \mathcal{D}_{\text{probe}}$  **do**
- 3:   Compute loss  $\mathcal{L}_{\text{SFT}}$  on  $\Theta(x_i)$
- 4:   Backpropagate gradients  $g_j = \frac{\partial \mathcal{L}_{\text{SFT}}}{\partial \theta_j}$
- 5:   Compute second-order Hessian approximations  $H_{jk}$
- 6:   **for**  $t = 1$  to  $L$  **do**
- 7:     **for** neuron  $j$  in layer  $t$  **do**
- 8:       Compute Shapley value  $\phi_j$  using Equation 4
- 9:        $\Phi_{t,j} \leftarrow \Phi_{t,j} + \phi_j$
- 10:     **end for**
- 11:   **end for**
- 12: **end for**
- 13: Average  $\Phi$  over samples
- 14: Select top- $T$  layers with highest total Shapley mass
- 15: Select top neuron groups of size  $G$  per chosen layer.
- 16: **return**  $\mathcal{N}$  using Equation 5

#### Algorithm 2: Two-Stage Contrastive Alignment of DIF

**Require:** Training set  $\mathcal{D}_{\text{train}} = \{(x_i, y_i, \mathcal{K}_i)\}$ , pretrained LLM  $\Theta$ , DIF neuron set  $\mathcal{N}$ , temperature  $\tau_{\text{cl}}, \tau_{\text{pcl}}$ , epochs  $E_1, E_2$ , weighting factor  $\lambda$

**Ensure:** Optimized  $g_{\text{align}}$  and prototype  $\mu$

- 1: **Step 0: DIF Embedding Extraction**
- 2: Initialize embedding set  $\mathcal{Z} \leftarrow \emptyset$
- 3: **for each**  $(x_i, y_i, \mathcal{K}_i) \in \mathcal{D}_{\text{train}}$  **do**
- 4:   Extract DIF embedding:  $\mathbf{z}_i \leftarrow \text{PROBE}(\Theta(x_i), \mathcal{N})$
- 5:   Store  $\mathbf{z}_i$  and metadata in  $\mathcal{Z} \leftarrow \mathcal{Z} \cup \{(\mathbf{z}_i, y_i, \mathcal{K}_i)\}$
- 6: **end for**
- 7: **Stage 1: Inter-KB Alignment**
- 8: **for epoch**  $e = 1$  to  $E_1$  **do**
- 9:   **for each** minibatch  $\{(\mathbf{z}_i, y_i, \mathcal{K}_i)\}_{i=1}^B$  **do**
- 10:     Compute aligned embeddings  $\mathbf{r}_i = g_{\text{align}}(\mathbf{z}_i)$
- 11:     Compute  $\mathcal{L}_{\text{cl}}$
- 12:     Update  $g_{\text{align}}$  parameters via backpropagation
- 13:   **end for**
- 14: **end for**
- 15: **Stage 2: Intra-KB Alignment**
- 16: Compute aligned embeddings  $\mathbf{r}_i = g_{\text{align}}(\mathbf{z}_i)$  for all  $i$
- 17: Cluster  $\{\mathbf{r}_i\}$  in  $\mathcal{K}_i$  to initialize prototypes  $\{\mu_m\}_{m=1}^M$
- 18: **for epoch**  $e = 1$  to  $E_2$  **do**
- 19:   **for each** minibatch  $\{(\mathbf{z}_i, y_i, \mathcal{K}_i)\}_{i=1}^B$  **do**
- 20:     Compute aligned embeddings:  $\mathbf{r}_i = g_{\text{align}}(\mathbf{z}_i)$
- 21:     Select nearest prototype to  $\mathbf{r}_i$  from  $\{\mu_m\}_{m=1}^M$
- 22:     Compute  $\mathcal{L}_{\text{cl}}$  and  $\mathcal{L}_{\text{pcl}}$
- 23:     Compute total loss:  $\mathcal{L} = (1-\lambda)\mathcal{L}_{\text{pcl}} + \lambda\mathcal{L}_{\text{cl}}$
- 24:     Update  $g_{\text{align}}$  parameters via backpropagation
- 25:   **end for**
- 26: **end for**
- 27: Recompute  $\mathbf{r}_i$  and update prototypes  $\mu$  by clustering
- 28: **return** Optimized  $g_{\text{align}}$  and prototypes  $\{\mu_m\}_{m=1}^M$

### Algorithm 3: Adaptive Prototype-Guided Routing

**Require:** Query  $q$ , trained encoder  $g_{align}$ , prototype set  $\{\mu_m\}_{m=1}^M$ , retrieval threshold  $\tau$ , top- $N$  selection size  $N$ , total slots  $T$

**Ensure:** Routing weights  $w_k$  for each knowledge base  $k$

- 1: Compute DIF embedding:  $\mathbf{z} \leftarrow \text{PROBE}(\Theta(q), \mathcal{N})$
- 2: Compute aligned embedding:  $\mathbf{q} \leftarrow g_{align}(\mathbf{z})$
- 3: Compute similarity scores:  $s_i \leftarrow \text{sim}(\mathbf{q}, \mu_i)$  for all  $i$
- 4: **if**  $\max_i s_i < \tau$  **then**
- 5:     **return** 0 ▷ Abstain from retrieval
- 6: **else**
- 7:     Identify top- $N$  prototypes:  $\mathcal{I} \leftarrow \text{TopN}(s, N)$
- 8:     **for** each knowledge base  $k$  **do**
- 9:         Compute slot count for KB  $k$ :

$$w_k \leftarrow \left\lfloor \frac{\sum_{i \in \mathcal{I}, k_i = k} s_i}{\sum_{k'} \sum_{i \in \mathcal{I}, k_i = k'} s_i} \cdot T \right\rfloor$$

- 10:     **end for**
- 11:     **return**  $[w_1, \dots, w_K]$
- 12: **end if**

## C. Prompt

In this section, we provide a detailed introduction to the prompts used in our framework:

### Dataset Construction Prompt

You are a knowledge expert tasked with creating a high-quality multiple-choice question based on the following text excerpt.

#### Requirements:

- Question should be clear, concise.
- Provide four answer options A, B, C, and D.
- Only one correct answer; the other three must be plausible but incorrect.
- Answer must be directly supported by chunk.
- Output the result strictly in JSON format.

#### Output Format:

```
{
  "question": "Question content",
  "options": {
    "A": "Option A",
    "B": "Option B",
    "C": "Option C",
    "D": "Option D"
  },
  "answer": "Correct letter (A-D)"
}
```

#### Text excerpt:

text      excerpt      here      (truncated      to  
MAX\_TEXT\_LENGTH if needed)

### Multi-Chunk Dataset Construction Prompt

You are an expert tasked with generating high-quality multiple-choice questions that integrates and synthesizes information across multiple chunks.

#### Requirements:

- The question **must require synthesis of information from all chunk\_num text excerpts**. Avoid disjointed or unrelated pairings.
- The stem should naturally integrate ideas, characters, events, or facts from the various excerpts into a cohesive question.
- Do not generate a question that simply juxtaposes unrelated content from different texts — such questions are considered invalid.
- Ensure only one correct answer exists, and all distractors are plausible based on full context.
- If the question cannot reasonably be formed without being disjointed, return false.
- Return the result in **strict JSON format**.

#### Output Format:

```
{
  "question": "Question content",
  "options": {
    "A": "Option A",
    "B": "Option B",
    "C": "Option C",
    "D": "Option D"
  },
  "answer": "Correct letter (A-D)"
}
```

Below are the chunk\_num related text excerpts. You must combine their information meaningfully in your question:

text      excerpt      here      (truncated      to  
MAX\_TEXT\_LENGTH if needed)

### DIF Probing Prompt

You are a domain-specific large language model connected to the following knowledge bases:

Knowledge Bases List: {database.list}

Given the query:

"{query}"

Please analyze and determine which knowledge base the query most likely belongs to. If it does not match any of the listed knowledge bases, respond with others.

#### Response Format:

Selected Knowledge Base: [name of the knowledge base or others]

### Prompt for Multiple-Choice QA

You are a professional multiple-choice QA assistant. Based on the provided context, answer the question by selecting the most appropriate option from A/B/C/D. Output only the option letter (A, B, C, or D) as the final answer; you may optionally add an explanation afterward.

#### **Prompt Format:**

<|im\_start|>system

You are a professional multiple-choice QA assistant. Please answer the question based on the given context by selecting one option (A, B, C, or D). Output only the option letter as the final answer, optionally followed by an explanation.

<|im\_end|>

<|im\_start|>user

Context: {context}

Question: {question}

Options:

A. {options.A}

B. {options.B}

C. {options.C}

D. {options.D}

Please select the best option based on the above information. Output only the option letter, for example: "B"

<|im\_end|>

<|im\_start|>assistant

Your answer here

<|im\_end|>

### Prompt for Short Answer QA

You are a professional QA assistant. Please answer the question based solely on the provided context. Follow the format below without omission:

#### **Prompt Format:**

<|im\_start|>system

You are a professional QA assistant. Answer the question based on the given context.

<|im\_end|>

<|im\_start|>user

Context: {context}

Question: {question}

<|im\_end|>

<|im\_start|>assistant

Your answer here

<|im\_end|>

### Prompt for LLM Judgment of Open-Ended Answers

You are a professional evaluator. Given the question, reference answer, and scoring criteria, please score the model-generated answer strictly from 0 to 10 (integer only). Return only the integer score without any extra text.

#### **Input:**

Question: {question}

Reference Answer: {standard\_answer}

Model Answer: {model\_answer}

#### **Scoring Criteria:**

1. Relevance: Does the answer directly address the question? (up to 4 points)
2. Accuracy: Is the content consistent with the reference answer? (up to 4 points)
3. Completeness: Does the answer cover key points in the reference? (up to 2 points)
4. Penalties:
  - Contains obvious errors: deduct 1–2 points
  - Completely unrelated or no answer: 0 points

#### **Examples:**

- Perfect and complete: 10 points
- Mostly correct but missing some details: 8–9 points
- Partially correct: score proportionally (e.g., 3/5 key points = 6 points)
- Irrelevant but no errors: no deduction
- Completely wrong or no answer: 0 points

Please strictly follow the criteria and return only an integer score:

## D. Retrieval Pipeline and Indexing Strategies

We adopt **FAISS** (Douze et al. 2024) for dense vector indexing across all retrieval settings. For the **Wikipedia (Wiki) knowledge base**, we follow the clustering strategy in Rop-Mura (Wu et al. 2025), partitioning 1M English passages into 10 semantically coherent knowledge bases. Passages are first embedded using `Qwen-embedding-v2` (Bai et al. 2023) for clustering, and subsequently indexed with `all-MiniLM-L6-v2` (Wang et al. 2020). For the **Medical (Med) knowledge base** (Zhao et al. 2025), we replicate the knowledge base construction from RAGRoute (Guerraoui et al. 2025), creating four distinct sources: PubMed, StatPearls, medical textbooks, and medical Wikipedia, each indexed using `all-βMiniLM-L6-v2`. For the **Private Enterprise Policy (PEP) knowledge base**, which contains internal Chinese-language company documents spanning four sub-knowledge bases, we utilize the `GTE-base-zh` encoder (Li et al. 2023) for indexing. For each query, DFAMS retrieves the top-10 documents from the dynamically selected source(s).

## E. Dataset Construction and Sampling Strategies

We conduct evaluations on three in-domain corpora and two out-of-domain (OOD) benchmarks.

**Wiki Dataset Construction.** The training set consists of 23,240 queries: among them, 2,100 queries explicitly require no retrieval, while 21,140 queries require retrieval of a single document from a single knowledge base. We deliberately exclude queries involving cross-knowledge-base or cross-document multi-segment retrieval to reduce data construction complexity, which also aligns better with practical scenarios. The test set contains 8,879 queries: 900 queries do not trigger retrieval, 969 queries require cross-knowledge-base multi-document collaboration, and 790 queries require same-knowledge-base multi-document collaboration. This setup is designed to verify the robustness of our method in realistic multi-knowledge-base scenarios.

**Med Dataset Construction.** Following a similar processing pipeline as Wiki, we construct the training and test sets for the medical domain. The training set includes only “no retrieval” or “single-knowledge-base single-segment” queries to reduce annotation costs. The test set additionally incorporates “cross-knowledge-base multi-segment” and “same-knowledge-base multi-segment” queries to evaluate the system’s generalization ability in realistic multi-knowledge-base collaboration scenarios. The test set contains 3,356 samples, with 438 requiring cross-knowledge-base multi-document collaboration and 823 requiring same-knowledge-base multi-document collaboration, to assess robustness in real multi-knowledge-base environments.

**PEP Dataset Construction.** We evaluate FR capabilities on a private enterprise policy dataset: the training set contains 2,088 samples, all querying single company policy documents from one knowledge base. The test set contains 344 samples, where queries are either categorized as “other” (requiring no retrieval) or require retrieval from a single knowledge base. Since PEP doesn’t have corresponding golden-label documents, recall statistics are not reported.

**OOD Dataset Construction.** Following the evaluation paradigm of RAGRoute (Guerraoui et al. 2025), we construct lightweight OOD test sets by extracting sub-questions from MMLU (Hendrycks et al. 2020) and MIRAGE (Xiong et al. 2024) that are most relevant to the topics covered by the existing four knowledge bases. For MMLU, we retain 1,222 questions that are potentially related to the WIKI knowledge base; for MIRAGE, we filter 1,546 open-domain QA samples with the highest entity co-occurrence with the four knowledge bases. Both subsets lack corresponding golden-label documents and are used solely to evaluate the model’s robustness and knowledge generalization under domain shift and non-retrieval conditions.

## F. Baseline Implementation Details

We evaluate six representative methods under the DFAMS benchmark. The implementation details of these baseline methods are as follows:

**No-RAG.** As a non-retrieval baseline, we directly apply the original LLM without any external knowledge.

**Merged-RAG.** There is no separation between individual knowledge bases — all content is integrated into a single, unified knowledge base and indexed together for retrieval.

**Prompt.** A knowledge bases selection baseline where a powerful 70B teacher model is used to classify which knowledge bases should be retrieved. This is necessary because smaller models (e.g., 7B) exhibit poor performance on explicit knowledge bases routing tasks. The 70B model performs knowledge bases classification via prompt-based reasoning. Based on the selected corpora, relevant documents are retrieved and then passed to a 7B LLM for final answer generation.

**CotPrompt.** A knowledge bases selection where a 70B teacher model is used to perform corpus routing, but with chain-of-thought (CoT) prompting (Wei et al. 2022). Compared to Prompt, this variant enhances reasoning by explicitly incorporating intermediate steps during knowledge bases classification and downstream answer generation.

**RopMura.** A recent joint retrieval and routing method (Wu et al. 2025). As our focus is on knowledge bases selection, we isolate and evaluate only the knowledge bases selection module. Multi-turn dialog components are disabled for fair comparison.

**RAGRoute.** For each knowledge bases, we train an MLP-based router whose architecture and training settings exactly match those of our Align-MLP, ensuring a fair comparison (Guerraoui et al. 2025). All methods share the same encoder and retriever: we use `all-MiniLM-L6-v2` for Wiki and Med, and `gte-base-zh` for PEP.

## G. Metric Definitions and Evaluation Configuration

We evaluate DFAMS using three complementary metrics:

**Cls Acc.** This metric measures whether the method correctly identifies the relevant knowledge base(s). A prediction is considered correct if it matches the ground-truth KB in single-source cases, outputs `Others` when no retrieval is required, or fully covers all gold KBs in multi-source cases.

**Recall.** This metric follows standard RAG evaluation and is computed over the Top-10 retrieved documents. It is calculated only for retrieval-triggering queries, and measures the proportion of gold documents that appear within the Top-10 retrieved results. Formally, it is defined as the number of retrieved gold documents divided by the total number of gold documents for a given query. Queries that do not require retrieval are excluded to better isolate and evaluate the retrieval component.

**QA.** This metric evaluates the final response quality. For multiple-choice questions, we extract the predicted option(s) (e.g., A/B/C/D) from the model output and compare them against the ground-truth answer. For open-ended queries, responses are scored by an LLM-based judge (Zheng et al.

2023) that assesses factual correctness and fluency. The score ranges from 0 to 10.

## H. Layer Attribution Analyses

In this appendix, we present supplementary results and analyses that support the findings discussed in Section 4.3. Specifically, Table 7 reports layer-wise attribution results on the PEP dataset without using the Align MLP. Layer 26 yields the highest Shapley value (1.1895) and also achieves the best classification accuracy (72.70%), suggesting it plays a critical role in capturing query-subdomain associations. Layer 27 ranks second in both Shapley score (0.3765) and accuracy (72.51%), further reinforcing the strong correlation between attribution values and downstream performance. In contrast, layers with lower Shapley scores—such as Layer 15 (0.0737)—correspond to substantially worse accuracy (27.83%). These results confirm the effectiveness of Shapley analysis in identifying semantically important layers.

Layer	Act	Grad ( $\times 10^{-6}$ )	Shapley	Cls Acc ( $\uparrow$ )
26	-10.19	1.030	<b>1.1895</b>	<b>72.70</b>
27	7.53	0.671	0.3765	72.51
23	2.15	0.724	0.1375	57.71
4	3.13	0.662	0.1357	56.61
3	3.89	0.641	0.1339	46.17
15	4.36	0.635	0.0737	27.83

Table 7: Layer-wise attribution results on the PEP dataset.

In addition, we compare three attribution metrics—Shapley values, forward activations (Act) (Xu et al. 2024), and gradient (Grad) (Zhang et al. 2023). Gradients are scaled by  $10^{-6}$  for readability. Among these metrics, Shapley consistently aligns with model performance: for instance, Layer 26 has both the highest Shapley score (1.1895) and top classification accuracy (72.70%). In contrast, Act and Grad provide less reliable signals. For example, Layer 15 receives relatively high Act and Grad values (4.36 and 0.635, respectively), yet performs poorly (27.83% accuracy), indicating a weak correlation between these metrics and actual task effectiveness. Similarly, Layer 3 shows moderately high Act (3.89) but achieves only 46.17% accuracy. These observations highlight the superior interpretability and layer-selection reliability of Shapley attribution in this setting.

## I. Effect of Backbone Model Size.

We evaluate DFAMS with Qwen2.5 models of 0.5B, 3B, and 7B parameters. As shown in Table 8, the 0.5B and 3B models achieve accuracy of 81.23% and 83.56%, and retrieval recall of 50.75% and 52.12%, respectively. Compared with the 7B model, the performance gap is relatively small, demonstrating that our framework can deliver strong performance even with smaller model sizes.

## J. Effect of Learning Rate

Table 9 shows the classification accuracy of DFAMS under varying learning rates. The model achieves the best per-

Backbone	Cls Acc ( $\uparrow$ )	Recall ( $\uparrow$ )
Qwen2.5-0.5B	81.23	50.75
Qwen2.5-3B	83.91	51.39
Qwen2.5-7B	<b>85.03</b>	<b>53.83</b>

Table 8: Performance of DFAMS with different backbone models on the Wiki dataset.

formance at a learning rate of  $1e-4$ , reaching 85.03% accuracy. Both larger ( $1e-3$ : 81.51%) and smaller ( $1e-5$ : 54.25%) learning rates lead to performance drops.

Learning Rate	$1e-3$	$5e-4$	$1e-4$	$5e-5$	$1e-5$
Cls Acc ( $\uparrow$ )	81.51	83.56	<b>85.03</b>	83.22	54.25

Table 9: Cls Acc of different learning rates using DFAMS.

## K. Experiment Environment

Experiments were conducted on a server equipped with dual Intel Xeon E5-2680 v4 CPUs (56 cores, 112 threads), 8 NVIDIA RTX 3090 GPUs (24GB each), and 377 GB of Main Memory. The operating system is Ubuntu 18.04.6 LTS. We used Python 3.11.10 with PyTorch 2.4.0, and managed packages using Conda 23.5.2.

## L. Data Ethics Statement

To evaluate the efficacy of our work, we conducted experiments using five datasets: Wiki, Med, PEP, MMLU, and MIRAGE. Except for PEP, all datasets are publicly available and used in accordance with their respective terms of use. PEP was obtained and used with proper authorization. No personally identifiable information was involved, and no human or animal subjects participated in this research.